Scattering patterns of self-assembled gyroid cubic phases in amphiphilic systems

Piotr Garstecki and Robert Hołyst
Institute of Physical Chemistry PAS and College of Science, Department III, Kasprzaka 44/52, 01-224 Warsaw, Poland

(Received 16 November 2000; accepted 23 April 2001)

We present scattering patterns (with surface contrast) for five triply periodic minimal surfaces of the $Ia3d$ cubic symmetry. We obtain a very good agreement between the numerically obtained spectrum and experimental patterns for the simple gyroid G structure. We show the scattering patterns for four gyroid GX1, GX2, GX3, and GX5 structures of a complex topology. We show how the scattering patterns change with increasing complexity of the unit cell of the structure. The spectra of the complex structures can give wrong estimates about the cubic cell parameter and even wrong establishment of the space symmetry group. Thus the correct recognition of the structure present in the system requires the analysis of the intensities of the peaks and comparison with numerically obtained spectra. © *2001 American Institute of Physics.* [DOI: 10.1063/1.1379326]

I. INTRODUCTION

The triply periodic minimal surfaces (TPMS) are found in various physical and biological systems. The G gyroid structure (see Fig. 1) of the $Ia3d$ symmetry is one of, if not the one, most commonly observed cubic phases. It is formed in diblock *AB* copolymer melts, where it is the surface dividing the *A* and *B* monomer rich regions.[1] The *Y*** structure, the analog of the G surface is found in compounds with the garnet structure $Ca_3[Al_2Si_3O_{12}]$, materials important for their applications as optoelectric color displays and magnetic bubble memory.[2] It has been also shown that the MCM-48 mesoporous materials exhibit $Ia3d$ symmetry.[3] In biological systems it is known that the intercellular lipid membranes can form the G structure.[4] There are many examples and technological applications of such systems; for example, polymerized self-assembled amphiphilic structures are used as mesoporous sieves, catalyst and material for producing contact lenses.

In our work we focus on the amphiphilic solutions. The gyroid self-assembled structure is formed by surfactants or lipids in mixtures with water. The first experimental observation of a triply periodic structure in amphiphilic system was conducted by Luzzati and Spegt.[5] They have identified the gyroid structure by the small angle x-ray scattering technique in several water/surfactant mixtures with the polar head regions marked by strontium ions. Since then the gyroid structure has been multiply discovered in both x-ray and neutron scattering experiments and confirmed by nuclear magnetic resonance (NMR)[6] and transmission electron microscopy.[7] The small angle x-ray (SAXS) and neutron (SANS) scattering experiments are commonly used to explore the symmetry and structure of amphiphilic mixtures.[8–11] Apart from the G structure, several other cubic phases with various symmetries and topologies have been discovered (see, for example, Refs. 12–16 or 17), but the list may still be incomplete. Theoretically, the world of triply periodic minimal self-assembled structures is almost infinitely rich. Recently many new simple and complex periodic structures of cubic symmetry have been found in simple Landau–Ginzburg models of ternary mixtures.[18] Since the $Ia3d$ symmetry is so common in nature it is very interesting if other than the simple gyroid cubic structures of this symmetry are formed in real systems, and if it is possible to determine their existence by present scattering techniques.

This paper is devoted to the presentation of the numerical calculations of the scattering patterns of the $Ia3d$ surfaces. Apart from the simple gyroid structure G we evaluate the spectra of the complex structures GX1, GX2, GX3, and GX5 (see Fig. 2). It is worth noting here that the GX1 surface has already been taken into account in the analysis of the mesoporous MCM-48 materials.[3] In Sec. II we describe the physical system of our interest and the numerical model used for evaluating the scattering intensity. Section III includes the comparison between the numerical spectrum of the simple gyroid structure and two experimental patterns, the scattering spectra for four topologically complex gyroid TPMS and discussion of the results. Section IV contains the conclusions.

II. THE SYSTEM AND THE MODEL

The amphiphilic construction of the surfactant molecules induces very complex behavior in mixtures with water and hydrocarbons. At high surfactant concentrations, the amphiphilic molecules form layers which separate oil and water rich regions. Apart from lamellar and hexagonal structures, these layers can form triply periodical surfaces of various cubic symmetries. The paradigm of triply periodic surface is a triply periodic minimal surface with zero mean curvature. The TPMS divide the volume into two continuous and separate subvolumes. In surfactant mixtures, two physical realizations of a minimal surface are possible. One is a direct phase in which a water film is centered on the surface and surfactant molecules are filling the two subspaces. The second case is an invert phase in which the surface is decorated

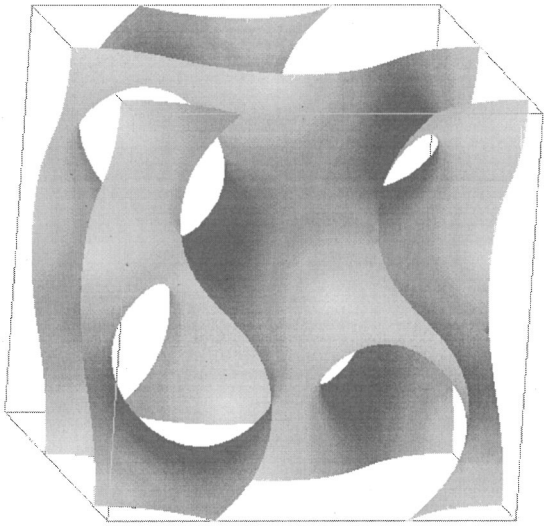

FIG. 1. The zero width–mathematical surface in the unit cell of the simple gyroid G structure.

by a bilayer of surfactant and oil, while the two subspaces are filled with water. In our work we focus on the invert phase. We calculate the scattering intensity assuming the bilayer contrast. It can be realized either in x-ray scattering experiments where it is due to the difference of electron densities of water and hydrocarbons, or in neutron scattering experiments when the hydrophobic surfactant chains are deuterated. This can be done without altering the mesoscopic structure of the system.[19]

The numerical model used to calculate the scattering intensities has been described in detail in Ref. 20. In brief, the TPMS were taken from the minimization procedure.[18] Then they were triangulated and each triangle was associated with a scattering rod pointing in the direction normal to the surface. This introduces the effects of the local curvature into the calculations. The scattering intensity $I(\mathbf{q})$ which is the

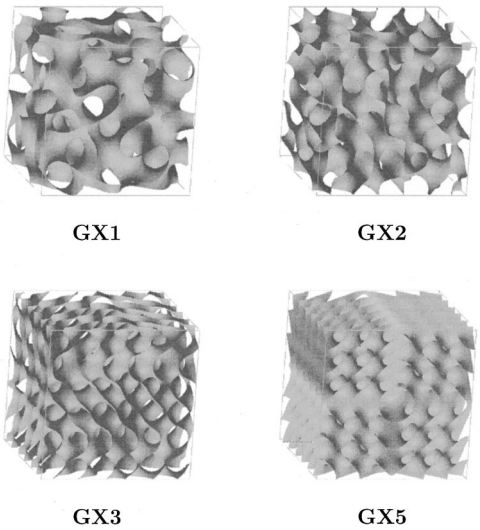

FIG. 2. The zero width–mathematical surfaces in the unit cells of the GX1, GX2, GX3, and GX5 structures. Better pictures of these and other cubic surfaces can be seen at http://www.ichf.edu.pl/Dep3.html.

TABLE I. Results of the comparison of the experimental scattering patterns from two systems – $C_{12}EO_2/H_2O$ (Ref. 14) (second column) and DDAB/H_2O/hydrocarbon (Ref. 15) (third column) with the intensities obtained numerically for the volume fraction of the bilayer $\phi_b=0.5$ (fourth column).

hkl	I_{exp} (Ref. 14)	I_{exp} (Ref. 15)	I_{num}
211	100	100	100
220	11	23	19
321	1	<1	1
400	1	<1	1
420	3	5	4
332	7	5	6

Fourier transform of the density–density correlation function reads as follows:

$$I(\mathbf{q})=\left(\sum_{j=1}^{N} s_j \cos(\mathbf{qr}_j)\frac{\sin[\mathbf{qn}_j(L/2)]}{\mathbf{qn}_j(L/2)}\right)^2 + \left(\sum_{j=1}^{N} s_j \sin(\mathbf{qr}_j)\frac{\sin[\mathbf{qn}_j(L/2)]}{\mathbf{qn}_j(L/2)}\right)^2, \quad (1)$$

where s_j is the surface area of the jth triangle, $\mathbf{r}_j$ is the position of the jth triangle's center, and $\mathbf{n}_j$ is a unit vector normal to the surface of the jth triangle. L is the width of the hydrocarbon part of the surfactant bilayer.

Besides the comparison with experimental patterns for the simple gyroid structure we are not computing the spectra for any particular system so we have set the width of the bilayer L to a typical value of 30 Å. The dimensionless width of the bilayer $l_a=L/a$ expressed as a fraction of the lattice parameter a is related to the volume fraction ϕ_B by the formula[13]

$$\phi_B=s^* l_a+\frac{\pi}{6}\xi_E l_a^3, \quad (2)$$

where s^* is the dimensionless surface area of one unit cell of the minimal base surface and ξ_E is the Euler characteristic given by the expression $\xi_E=2(1-g)$, where g is the genus. Setting the volume fraction ϕ_B to a reasonable value of 0.5 allows us to extract the l_a parameter and the lattice constant $a=(L=30\ \text{Å})/l_a(\phi_B=0.5)$.

III. RESULTS

A. The simple gyroid G surface

In order to check the accuracy of the model we have compared the numerically obtained scattering pattern of the simple gyroid G structure with the experimental spectra of two systems – $C_{12}EO_2$/water[14] and didodecyldimethylammonium bromide/water/hydrocarbon.[15] The numerical hkl intensities have been multiplied by the multiplicity factor. In both experiments the scattering intensities were collected on two-dimensional detectors. Before comparing the experimental intensities with those obtained numerically, we have Lorentz corrected them with an appropriate Lorentz-polarization factor. Data contained in Table I shows a very good agreement between the experimental and numerical intensities. It is quite important to note here that the structure

from the second experimental pattern have not been determined in Ref. 15. If not the infeasible values of the surface area per surfactant for the F-RD structure, authors would have associated it with the $Fm\bar{3}m$ symmetry group. This was due to the lack of the $\sqrt{14}$ reflection permitted by the $Ia\bar{3}d$ symmetry. Our calculations show that this is solely the effect of the low structure factor for the 321 reflection and low resolution of the experimental setup.

B. The complex gyroid surfaces

All of the scattering spectra for GX1, GX2, GX3, and GX5 structures are in excellent agreement with the $Ia\bar{3}d$ space group. The hkl peaks prohibited by the reflection conditions are 5–6 orders of magnitude smaller than the allowed peaks. Still the structure factor of these surfaces makes some of the allowed peaks also very weak. This is particularly interesting in the case of the complex structures, where due to this phenomena the low order hkl peaks are small and the intensity is shifted towards the longer scattering vectors and bigger hkl indices. In order to simulate the powder diffraction data, the intensities have been multiplied by the full multiplicity factor.

To present typical scattering data, that could be obtained in an experiment, we have convoluted the delta hkl peaks with the Gaussian resolution function $R(\mathbf{q}) = \exp(-|\mathbf{q}|^2/2\sigma^2)$ where σ is the experimental resolution in inverse angstroms. This way, the experimental intensity can be written as follows:

$$I_{\exp}(q) = \frac{1}{\sqrt{2\pi\sigma^2}} \sum_{hkl} \exp\left[\frac{-|\mathbf{q}_{hkl}-\mathbf{q}|^2}{2\sigma^2}\right] I(\mathbf{q}_{hkl}), \qquad (3)$$

where $I(\mathbf{q}_{hkl})$ is given by Eq. (1).

The experimental resolution σ depends on the apparatus. Even though there are very sensitive two-dimensional detectors, for example, Ref. 21 ($\sigma < 1\times10^{-3}$ Å^{-1}), still many experiments are carried out on apparatus with worse resolution, for example, Refs. 22 ($\sigma \approx 3\times10^{-3}$ Å^{-1}), 23 ($\sigma \approx 7\times10^{-3}$ Å^{-1}), 24 ($\sigma \approx 3\times10^{-3}$ Å^{-1}), or 25 ($\sigma \approx 3\times10^{-3}$ Å^{-1}). The problem with low resolution is very evident in the data collected with one-dimensional detectors that are commonly used to explore the structure of amphiphilic mixtures and to track the phase transitions in these systems (in time resolved techniques), for example, Ref. 14.

In our work we have set the resolution to $\sigma = 2\times10^{-3}$ Å^{-1}. We think that this is a reasonable value to present the scattering patterns of the explored structures and to check what kind of data is experimentally accessible.

All of the spectra presented below have been calculated for typical values of the volume fraction of the bilayer ($\phi_B = 0.5$) and the bilayer width ($L = 30$ Å). The spectrum of the simple gyroid G structure has been shown in Ref. 26. One can also find the spectra of complex surfaces of other space groups there. It is enough to say here that the scattering pattern for the simple gyroid G structure contains few well-resolved hkl reflections ($\sqrt{6}, \sqrt{8}, \sqrt{14}, \sqrt{16}, \sqrt{6}, \sqrt{20}$, and $\sqrt{22}$). These peaks do not merge and the function $I_{\exp}(q)$ [Eq. (3)] bears the same amount of information as $I(\mathbf{q}_{hkl})$ [Eq. (1)]. Thus the experimentally accessible spectrum can be correctly indexed to the $Ia\bar{3}d$ symmetry group allowing correct prediction about the structure and its cell parameter $a = 173$ Å.

In the case of the complex gyroid structures due to the set resolution $\sigma = 2\times10^{-3}$ Å^{-1} the hkl reflections merge and form smaller number of experimentally visible peaks. These are simulated by the maxima of the function $I_{\exp}(q)$ [Eq. (3)]. To check whether these maxima can be indexed to the correct $Ia\bar{3}d$ space symmetry group we have conducted the indexing procedure. First an acceptable error δ_q in measurement (or shift due to experimental details) in the location of the scattering peaks q_n is established. Each scattering peak is assumed to lay between two values: $q_n^- = q_n - \delta_q$ and $q_n^+ = q_n + \delta_q$. Then all the locations are reduced to the ratios of their location to the location of the first peak q_0 in a way that assumes the largest possible error. That is,

$$\tilde{q}_n^- = \frac{q_n^-}{q_0^+}, \quad \tilde{q}_n^+ = \frac{q_n^+}{q_0^-}, \qquad (4)$$

and

$$\tilde{q}_n^- < \tilde{q}_n < \tilde{q}_n^+ . \qquad (5)$$

Now $(\tilde{q}_0)^2$ is integer and equal to 1. If the peaks can be indexed to any symmetry group, all the $(\tilde{q}_n)^2$ values have to be integer. Then the squares of all reduced locations are multiplied by a growing integer M and we check whether any integer $N_n = h^2+k^2+l^2$ lay between $M(\tilde{q}_n^-)^2$ and $M(\tilde{q}_n^+)^2$. If it is true for all the peaks, we check whether the set of the $\sqrt{N_n}$ spacings are allowed by a given symmetry group. Of course there might be more than one integer M, that leads to spacings allowed by some symmetry group. If so, the lowest one is chosen.

Since the space group of each structure is known, the object of ascribing the indices to the experimental peaks was not to find the correct group, but to check if the experimentally accessible peaks could be indexed to a wrong group. Then we have taken into account only three space symmetry groups commonly found in amphiphilic mixtures, $Pn\bar{3}m$, $Im\bar{3}m$, and $Ia\bar{3}d$.

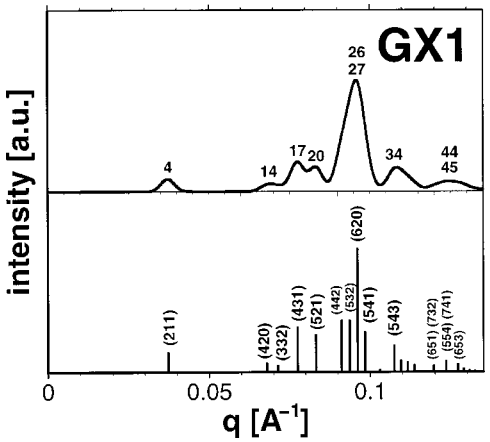

FIG. 3. The scattering pattern for the GX1 structure. In the bottom part of the figure the true hkl reflections are shown as delta peaks. The upper part contains the experimentally accessible intensity curve simulated by the function $I_{\exp}(q)$ Eq. (3). The square roots of the numbers N_n above the experimentally visible peaks give the lowest possible assignment of their spacings.

TABLE II. Results of the indexing procedure of the spectrum of the GX1 gyroid structure. The first column shows the locations of the experimentally accessible peaks. The second column contains the set of the square roots of the integers $N_n(M(\tilde{q}_n^-)^2<N_n<M(\tilde{q}_n^+)^2)$ for the lowest possible value of $M=4$ and $\delta_q=0.001q_0$ (see text). These spacings are allowed by the $Pn3m$ space symmetry group. In the last column the true hkl reflections that form the experimentally visible peaks are presented.

q_n (Å^{-1})	$\sqrt{N_n}$	hkl
0.037	$\sqrt{4}$	221
0.069	$\sqrt{14}$	420,332
0.077	$\sqrt{17}$	431
0.083	$\sqrt{20}$	521
0.095	$\sqrt{26}$ or $\sqrt{27}$	442,532
		620,541
0.108	$\sqrt{34}$	543,640,633
		721,552,642
0.124	$\sqrt{44}$ or $\sqrt{45}$	651,732,554
		741,820,653
		822,660,831
		743,662

Figure 3 presents the scattering spectrum of the GX1 structure. The delta peaks shown in the bottom part of the figure represent the hkl reflections evaluated numerically. The upper section of the figure presents the experimentally accessible spectrum — function $I_{\mathrm{exp}}(q)$ [Eq. (3)]. The first peak 211 is well distinguished, yet the 442, 532, 620, and 541 peaks merge into one experimentally visible peak. This means the loss of the information about the structure. Table II includes the locations of the seven experimentally visible peaks and the indices of the hkl peaks that form them. For the smallest error $\delta_q=0.001q_0$ in the location of the experimentally visible peaks the indexing procedure gives the following spacings: $\sqrt{4}, \sqrt{14}, \sqrt{17}, \sqrt{20}$, ($\sqrt{26}$ or $\sqrt{27}$), $\sqrt{34}$, ($\sqrt{44}$ or $\sqrt{45}$), which are allowed by the $Pn3m$ space group. This indexation gives also wrong establishment of the cell parameter a:

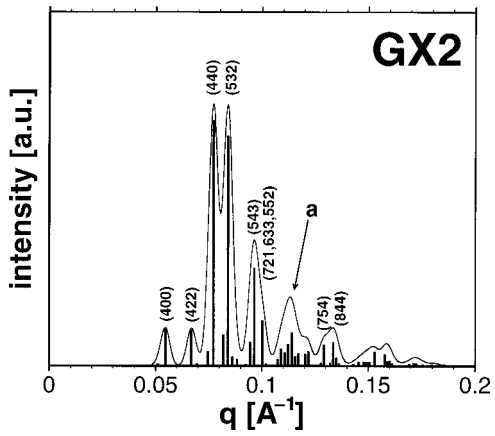

FIG. 4. The scattering pattern for the GX2 structure. The delta peaks represent the true hkl reflections of the GX2 structure, while the thin line shows the experimentally accessible intensity curve. The peak denoted by the letter **a** composes from the following hkl peaks: 800, 820, 653, 822, 743, 752, 840.

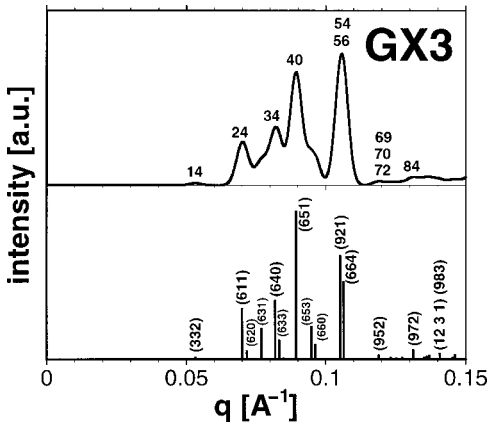

FIG. 5. The scattering pattern for the GX3 structure (see legend of Fig. 3).

$$a=\frac{2\pi\sqrt{4}}{q_0=0.037}=340, \tag{6}$$

while in reality $a=415$ Å. Allowing bigger error ($\delta_q=0.01q_0$) in the locations of the peaks one can fit the data to the $Ia3d$ symmetry. The indices of the first peak would then be established as 321 ($\sqrt{14}$) and the cubic lattice parameter as $a=635$ Å. This example clearly shows that with the given resolution, the symmetry and size of the GX1 structure could not be identified correctly.

Figure 4 shows the scattering pattern of the GX2 structure. Again, as in the case of the GX1 surface, the hkl delta peaks merge into smaller number of experimentally visible peaks. Yet the maxima of the function $I_{\mathrm{exp}}(\mathbf{q})$ lay close to the most pronounced underlying hkl reflections. The experimentally accessible intensity curve can be indexed correctly to the sequence of $\sqrt{16}, \sqrt{24}, \sqrt{32}, \sqrt{38}, \sqrt{50}$, etc., permitted by the $Ia3d$ space symmetry group. This gives the correct evaluation of the cell parameter as $a=460$ Å.

Figure 5 presents the scattering spectrum of the GX3 structure. The experimentally visible peaks can be indexed as $\sqrt{14}, \sqrt{24}, \sqrt{34}, \sqrt{40}$, ($\sqrt{54}$ or $\sqrt{56}$), ($\sqrt{69}, \sqrt{70}$, or $\sqrt{72}$), and $\sqrt{84}$. These spacings are permitted by both $Pn3m$ and $Im3m$ symmetry groups. Yet none of them is the correct symmetry group $Ia3d$. This assignment gives $a=444$ Å while in reality $a=554$ Å. The last examined structure is GX5 (Fig. 6).

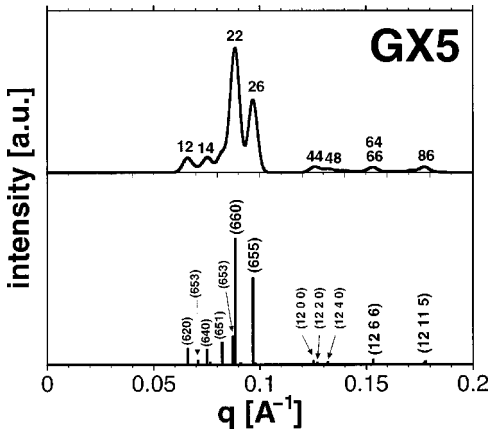

FIG. 6. The scattering pattern for the GX5 structure (see legend of Fig. 3).

Again the true hkl reflections merge causing severe loss of information. The spacings of the experimentally accessible peaks — $\sqrt{12}, \sqrt{14}, \sqrt{22}, \sqrt{26}, \sqrt{44}, \sqrt{48}$, ($\sqrt{64}$ or $\sqrt{66}$), and $\sqrt{86}$ — give wrong estimates both about the symmetry ($Im3m$ instead of $Ia3d$) and the cubic lattice parameter ($a = 330$ Å instead of the correct value $a = 602$ Å).

IV. CONCLUSIONS

We have presented scattering patterns of four topologically complex cubic structures of the $Ia3d$ symmetry. The accuracy of the numerical model used to evaluate the scattering intensities have been checked by comparison of the numerical pattern of the simple gyroid G structure with two experimental spectra.[14,15] A very good agreement of the data ensures the relevancy of the model. Furthermore, in one of the two examples, it was the comparison of the numerical pattern with experimental data that allowed correct and unambiguous determination of the structure.

We have demonstrated that the size and complexity of the unit cells of the GX1, GX2, GX3, and GX5 gyroid structures makes it practically impossible to determine their symmetry correctly without the analysis of the relative intensities of the peaks. Out of these four explored structures, the experimentally accessible intensity curve of only one (GX2) has been indexed to the $Ia3d$ space group. In the case of all the other three surfaces, the true Bragg reflections have merged to form a fewer number of visible peaks. The intensity curves do not bear enough information about the structures to enable correct determination of the symmetry and lattice parameters.

In the case of the simple cubic structures the strongest reflections are those of the lowest hkl indices. It can be easily explained by the fact, that the bilayer density–density correlation function acquires maximum at the lengths comparable with the lattice parameter. In the case of the complex structures, because of the complexity of the motive in the unit cell, the correlation length is much smaller than the unit cell parameter. The intensity is shifted towards longer scattering vectors and higher hkl indices. This phenomenon has been presented here and in Ref. 26. Most of the theoretically predicted minimal surfaces[18] have not yet been discovered. Still some already published scattering patterns indicate existence of cubic structures with a topologically complex motive in the unit cell. For example, the scattering spectrum of the system dimyristoylphosphatidylcholine/myristic acid[27] composes of the peaks indexing to the sequence of $\sqrt{3}, \sqrt{8}, \sqrt{11}, \sqrt{12}, \sqrt{16}, \sqrt{19}, \sqrt{24}, \sqrt{27}, \sqrt{32}, \sqrt{35}$. The scattering intensity in this pattern is centered in the higher order peaks: $\sqrt{8}(I_{220} \approx 45)$, $\sqrt{11}(I_{311} \approx 100)$, and $\sqrt{12}(I_{222} \approx 25)$, while the first peak $\sqrt{3}$ is very weak ($I_{111} \approx 5$). As it was shown in this paper, the analysis of the scattering patterns of complex surfaces can be very difficult. The experimentally accessible peaks may not uncover the true structure of the system.

The self-assembled triply periodic structures have more and more technological applications. For example, the complex structures could be very useful as templates for the photonic band gap materials. The theoretical analysis of the electromagnetic properties of the TPMS based systems[28] prove that the higher the complexity of the unit cell, the greater the probability of forming a complete three-dimensional photonic band gap and the richer is the photonic band structure. Thus the correct identification of the complex TPMS in amphiphilic and polymer systems may play a crucial role. Hopefully the theoretical and numerical evaluation of their scattering spectra will come in handy giving predictions about the relative intensities of the visible peaks.

ACKNOWLEDGMENT

This work has been supported by the KBN Grant No. 2P03B12516.

[1] D. A. Hajduk, P. E. Harper, S. M. Gruner, C. C. Honeker, E. L. Thomas, and L. J. Fetters, Macromolecules **28**, 2570 (1995).
[2] H. G. von Schnering and R. Nesper, Angew. Chem. **26**, 1059 (1987).
[3] P. I. Ravikovitch and A. V. Neimark, Langmuir **16**, 2419 (2000).
[4] T. Landh, FEBS Lett. **369**, 13 (1995).
[5] V. Luzzati and P. A. Spegt, Nature (London) **215**, 701 (1967).
[6] B. Lindman, K. Shinoda, U. Olsson, D. Anderson, D. Karlstrom, and H. Wennestrom, Colloids Surface **38**, 205 (1989).
[7] E. L. Thomas, D. B. Alward, D. J. Kinning, D. C. Martin, D. L. Handlin, and L. J. Fetters, Macromolecules **19**, 2197 (1986).
[8] P. C. Mason and B. D. Gaulin, Phys. Rev. E **59**, 3361 (1999).
[9] R. Gamez-Corrales, J. F. Berret, L. M. Walker, and J. Oberdisse, Langmuir **15**, 6755 (1999).
[10] W. A. Hamilton, P. D. Butler, J. B. Hayter, L. J. Magid, and P. J. Kreke, Physica B **221**, 309 (1996).
[11] M. B. Sjobom, H. Edlund, and B. Lindstrom, Langmuir **15**, 2654 (1999).
[12] D. C. Turner, Z. G. Wang, S. M. Gruner, D. A. Mannock, and R. N. McElhaney, J. Phys. II **2**, 2039 (1992).
[13] P. Strom and D. M. Anderson, Langmuir **8**, 691 (1992).
[14] S. S. Funari and G. Rapp, J. Phys. Chem. B **101**, 732 (1997).
[15] P. J. Maddaford and C. Toprakcioglu, Langmuir **9**, 2368 (1993).
[16] U. Peter, S. Konig, D. Roux, and A. M. Bellocq, Phys. Rev. Lett. **76**, 3866 (1996).
[17] P. Alexandridis, U. Olsson, and B. Lindman, Langmuir **14**, 2627 (1998).
[18] W. T. Góźdź and R. Hołyst, Phys. Rev. E **54**, 5012 (1996).
[19] B. Svensson, U. Olsson, P. Alexandridis, and K. Mortensen, Macromolecules **32**, 6725 (1999).
[20] P. Garstecki and R. Hołyst, J. Chem. Phys. **113**, 3772 (2000).
[21] A. Angelova, R. Ionov, M. H. J. Koch, and G. Rapp, Arch. Biochem. Biophys. **378**, 93 (2000).
[22] P. Barois, D. Eidam, and S. T. Hyde, J. Phys. (Paris), Colloq. **C7**, 25 (1990).
[23] S. Radiman, C. Toprakcioglu, L. Dai, A. R. Faruqi, R. P. Hjelm, Jr., and A. de Vallera, J. Phys. (Paris), Colloq. **C7**, 375 (1990).
[24] X. Wang and P. J. Quinn, Biophys. Chem. **80**, 93 (1999).
[25] S. L. Keller, S. M. Gruner, and K. Gawrisch, Biochim. Biophys. Acta **1278**, 241 (1996).
[26] P. Garstecki and R. Hołyst, Phys. Rev. E (in press) 2001.
[27] R. Koynova, B. Technov, and G. Rapp, Chem. Phys. Lipids **88**, 45 (1997).
[28] L. Martin-Moreno, F. J. Garcia-Vidal, and A. M. Somoza, Phys. Rev. Lett. **83**, 73 (1999).